

PAPER DETAILS

TITLE: Is there a relationship between Diffusion Weighted Imaging and Histopathological Type in Brain Metastases Due to Breast Cancer?

AUTHORS: Seyhmus Kavak,Nazan Çiledag

PAGES: 133-139

ORIGINAL PDF URL: <https://dergipark.org.tr/tr/download/article-file/3348619>

Is there a relationship between Diffusion Weighted Imaging and Histopathological Type in Brain Metastases Due to Breast Cancer?

Şeyhmus KAVAK¹, Nazan ÇİLEDAĞ²

ABSTRACT

Aim: The aim of this study is to evaluate the relationship between diffusion-weighted imaging (DWI) properties and apparent diffusion coefficient (ADC) values of metastases with the histological type of breast cancer in patients with breast cancer-related brain metastasis.

Material and Methods: Between May 2008 - April 2011, 57 female patients who had been previously diagnosed with breast cancer in the radiology clinic were included in the study. Cases with invasive ductal carcinoma were considered group 1 (46 patients, 89 lesions) and cases with invasive lobular, comedo carcinoma and papillary cribriform carcinoma were considered group 2 (11 patients, 25 lesions). ADC values in both groups were compared by statistical analysis methods.

Results: In group 1; 37 lesions (41.57%) and in group 2; 13 lesions (52%) included cystic component. In the group of invasive ductal carcinoma 48 lesions (53.92%) and 18 lesions (72%) of second group included peritumoral edema. The mean ADC value of the solid component of metastases (group1: 1.105x10⁻³mm²/s, group2: 1.099x10⁻³mm²/s) was higher than the average ADC value of normal brain parenchyma (group1: 0.790x10⁻³mm²/s, group2: 0.801x10⁻³mm²/s), and was statistically significant (p<0.001). In the comparison between the groups, no statistically significant difference was found between the mean ADC values of the solid components of metastases (p= 0.931).

Conclusion: In our study, mean ADC values in brain metastases due to breast cancer were significantly higher than normal brain parenchyma. However, no statistically significant difference was found in the comparison of ADC values of the groups formed according to histopathological subtypes.

Keywords: Breast carcinoma; diffusion-weighted imaging; apparent diffusion coefficient

Meme Kanserine Bağlı Beyin Metastazlarında Difüzyon Ağırlıklı Görüntüleme ile Histopatolojik Tip Arasında Bir İlişki Var mı?

ÖZ

Amaç: Bu çalışmanın amacı, meme kanserine bağlı beyin metastazı olan hastalarda meme kanserinin histolojik tipi ile metastazların difüzyon ağırlıklı görüntüleme (DAG) özellikleri ve görünür difüzyon katsayısı değerleri (ADC) arasındaki ilişkiyi değerlendirmektir.

Gereç ve Yöntemler: Mayıs 2008-Nisan 2011 tarihleri arasında daha önce radyoloji kliniğinde meme kanseri tanısı almış 57 kadın hasta çalışmaya dahil edildi. İnvaziv duktal karsinomlu olgular grup 1 (46 hasta, 89 lezyon) ve invaziv lobüler, komedo karsinom ve papiller kribriform karsinomlu olgular grup 2 (11 hasta, 25 lezyon) olarak değerlendirildi. Her iki gruptaki ADC değerleri istatistiksel analiz yöntemleri ile karşılaştırıldı.

Bulgular: Birinci grupta; 37 lezyon (%41,57) ve grup 2'de; 13 lezyon (%52) kistik komponent içeriyordu. İnvaziv duktal karsinom grubunda 48 lezyon (%53,92), ikinci grupta 18 lezyon (%72) peritümöral ödem içeriyordu. Solid metastazlarda ortalama ADC değeri (grup 1: 1,105x10⁻³mm²/s, grup2: 1,099 x10⁻³mm²/s normal beyin parankiminin ortalama ADC değerinden (grup 1: 0,790 x10⁻³mm²/s, grup2: 0,801 x10⁻³mm²/s) yüksekti ve fark istatistiksel olarak anlamlıydı (p<0.001). Gruplar arası karşılaştırmada solid metastazların ortalama ADC değerleri arasında istatistiksel olarak anlamlı fark bulunmadı (p=0,931).

Sonuç: Çalışmamızda meme kanserine bağlı beyin metastazlarında ortalama ADC değerleri normal beyin parankimine göre anlamlı olarak yüksek bulundu. Ancak histopatolojik alt tiplere göre oluşturulan grupların ADC değerleri karşılaştırıldığında istatistiksel olarak anlamlı fark bulunmadı.

Anahtar Kelimeler: Meme kanseri; difüzyon ağırlıklı görüntüleme; görünür difüzyon katsayısı.

1 University of Health Sciences, Gazi Yasargil Training and Research Hospital, Department of Radiology, Diyarbakir, Türkiye.

2 Ankara Oncology Education and Research Hospital, Department of Radiology, Ankara, Türkiye.

Sorumlu Yazar / Corresponding Author Şeyhmus Kavak, e-mail: s.ozgurkavak@hotmail.com

Geliş Tarihi / Received: 20.08.2023, Kabul Tarihi / Accepted: 07.01.2024

INTRODUCTION

Breast cancer is the most common cancer among women. 10-30 % of patients diagnosed with breast cancer have brain metastasis (1,2). Today, magnetic resonance imaging (MRI) is the most commonly used and recommended modality for the evaluation of central nervous system (CNS) metastasis associated with breast cancer during the follow-up period. Diffusion-weighted magnetic resonance imaging (DWI) is a relatively new and precise MRI technique compared to conventional MRI, and it relies on the detection of the microscopic motion of water molecules (Brownian movement). The use of advanced MRI techniques, such as DWI, provides important findings in distinguishing malignant and benign masses and detecting some diseases (3-7). It also helps to differentiate pathologies that lead to similar imaging features in conventional MRI (8-11).

Many types of cancer cause CNS metastasis. There are few studies in the literature showing the radiological features of breast cancer CNS metastases. However, there is no comprehensive study revealing the characteristics of primary breast cancer metastases according to their histological subtypes. We aimed to reveal the DWI characteristics of brain metastases of primary breast cancer and to determine the correlation or difference in terms of ADC values measured between groups formed according to histopathological subtypes of breast cancer.

MATERIAL AND METHODS

Patient Selection: The fifty-seven female patients who developed brain metastasis due to primary breast cancer between May 2008 and April 2011 were included in this study. Of the patients included in the study, 46 were diagnosed with invasive ductal carcinoma, 7 with invasive lobular carcinoma, 2 with invasive papillary carcinoma,

and 2 with comedo carcinoma. Forty-six patients with invasive ductal carcinoma were considered group 1, and 11 patients with other histopathological types were considered group 2. MRI examinations were performed on breast cancer patients during the follow-up period due to complaints such as headache, dizziness, nausea, vomiting, loss of strength in the extremities, visual impairment, imbalance, and lethargy. This study was derived from the specialty thesis and was approved by the ethics committee of our hospital without the need for informed consent due to its retrospective nature ((Education Planning Commission ID: 2011/318).

Obtaining Brain MRI and Technical Parameters: All MRI sequences were obtained by a 1.5 T MRI scanner with a high-speed gradient (General Electric, Signa Excite HDx, Milwaukee, WI, USA). On sagittal plane, T2 weighted sequences, on axial plane T1W, T2W and FLAIR sequences, on coronal plane T2 weighted sequence and following 0.1 mmol/kg gadolinium administration, on coronal and axial planes T1 weighted sequences were applied as standard in all cases. For T1 weighted, T2 weighted and FLAIR sequences, TR/TE values were 600/10.9 ms, 3960/81.8 ms, and 8802/90.4 ms. FOV: 24x24cm, respectively, the thickness of the section was: 5mm, NEX:1, and gap:1.5mm. DWI images were obtained using a single-shot spin echo, echo-planar imaging (EPI) sequence. The gradient 'b' factor was 1000 mm²/s. For DWI images, the parameters were TR:6000ms; TE:105 ms; FOV: 24x24cm; NEX:2; thickness of section:5,5mm. For DWI, the duration of imaging was 32 seconds. All DWI images were sent to the workstation (Advantage Windows, software version 4.4, GEMedical Systems). In all cases, the mean area of 34-96 mm² circular "region of interest" (ROI) was inserted into the lesions. The ROI insertion process was performed on ADC maps (Figure 1).

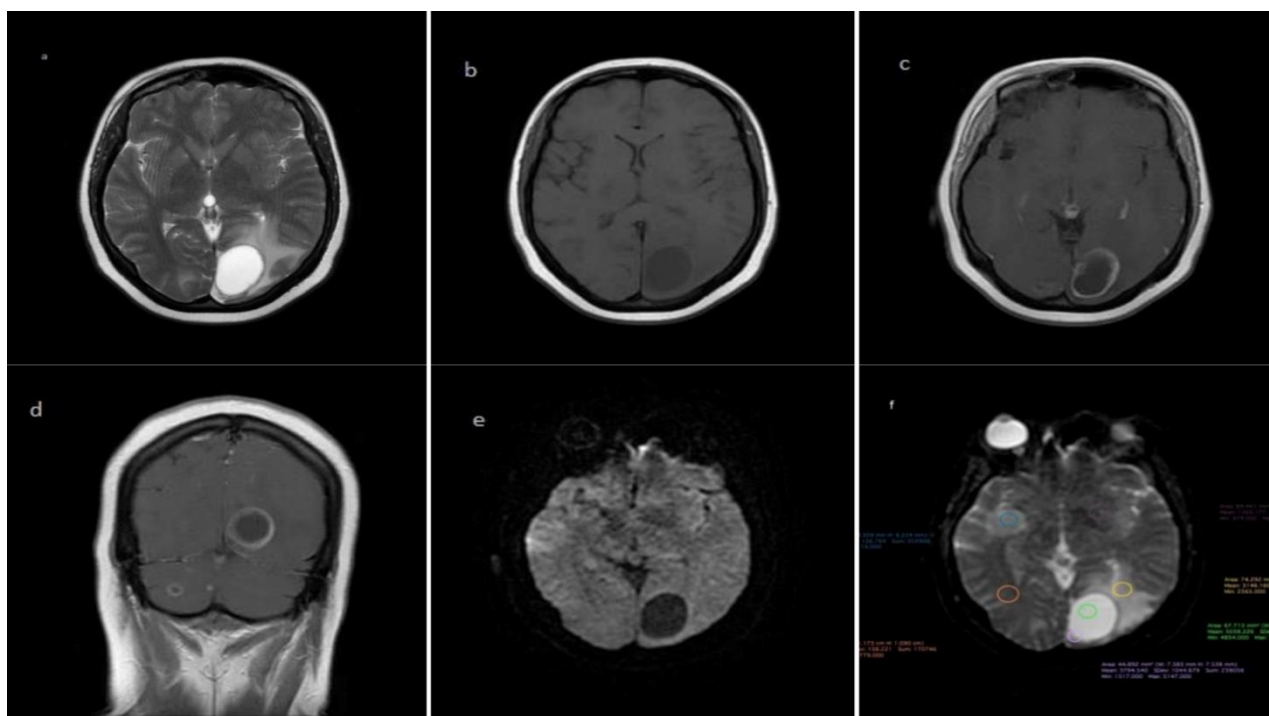


Figure 1. a-f. MR images of the left occipital lobe metastatic lesion (a- axial T2, b- axial T1, c-axial T1C+, d-Coronal T1C+, e-DWI and f-ADC map)

Interpretation of Brain MRI: Conventional contrast-enhanced MRI and DWI images were obtained from all cases, and ADC was measured from 114 possible metastatic lesions. Anatomical distribution, number of lesions, accompanying edema, presence of cystic component, contrast enhancement pattern, presence of bleeding findings and signal intensity were evaluated in the lesions in the brain parenchyma evaluated as metastatic. Images were evaluated by two radiologists, and in case of conflict, discussion and consensus were obtained. In all cases, measurements were performed on metastatic solid area, cystic components if any, areas with solid and cystic components and the same levels of normal parenchyma area on the contralateral lobe (Figure 2). ADC maps were calculated by the MRI system automatically and expressed as mm²/s. By placing the ROI, measurements were made from the solid component of all lesions, the cystic component if any, and the intact parenchyma tissue. In addition, measurements were made to include solid and cystic components. The mean ADC values were then calculated ADC values were compared by statistical analytic methods on the lesion, cystic component, if any, and normal tissue. Six of the patients (10.52%) who had been suspected of having metastasis on MRI had undergone surgery for histopathological evaluation. Histopathological confirmation was not required since the MRI findings of the remaining 51 (89.47%) patients were considered to be compatible with the metastasis of primary breast cancer. Chemotherapy/radiotherapy protocols were applied to these patients.

Statistical Analysis

Data were analyzed by IBM SPSS for Windows 11.5 package program. Shapiro Wilk test was used to verify whether the distribution of continuous variables is close to normal. P-value >0.05 was considered statistically significant for the results. Nonparametric tests were used for variables that did not meet this condition. Descriptive statistics were shown as mean ± standard deviation or

median (min-max) for continuous variables and categorical variables as number and percent (%) of cases. The significance of the difference between the groups in terms of means was investigated with Student's t test, and the significance of the difference in terms of median values was investigated with the Mann-Whitney U test when the number of independent groups was two. Whether there was a statistically significant difference between the groups in terms of ADC levels was evaluated using the Mann-Whitney U test. The existence of a statistically significant difference between the solid part, cystic part and normal parenchyma ADC levels among the groups was evaluated using the Wilcoxon Sign test. Categorical variables were examined using Pearson's Chi-Square or Fisher's Exact test. P-value <0.05 was considered statistically significant for the results.

RESULTS

The mean age of the patients was 43.79±10.1 years, and it was 43.93±10.3 in group 1 and 43.24±9.2 in group 2. There was hypointensity on DWI in 41 (46.06%) metastatic lesions in the invasive ductal carcinoma group and 11 (44%) metastatic lesions in group 2. No significant difference was found between the two groups in terms of DWI signal intensity (p=0.882). Which consisted of invasive ductal carcinoma cases, 37 (41.57%) metastatic lesions in group 1, and 13 (52%) metastatic lesions in group 2 included a cystic component (p= 0.508). In the group of invasive ductal carcinoma 48 lesions (53.92%) and 18 lesions (72%) of second group included peritumoral edema. In the comparison between the two groups, no statistically significant difference was found in parameters such as peritumoral edema, cystic component, and distribution of multi-lobe metastases. The enhancement pattern of metastatic lesions was predominantly heterogeneous in both groups. Heterogeneous enhancement was detected in 50 (56.17%) lesions in group 1 and in 18 (72%) lesions in group 2 (p=0.041) (Table 1).

Table 1. Demographic and clinical features of cases according to diagnostic groups

Variables	*Group I (n=46)	**Group II (n=11)	p-value
Age (years)	43.93±10.3	43.24±9.2	0.847
Number of Lobes			0.493
Single	22 (47.82%)	4 (36.36%)	
Multiple	24 (52.17%)	7 (63.63%)	
Metastasis Time (months)	44.72(7-133)	48.43(11-109)	0.893
Analyzing metastasis	*Group I (n=89)	**Group II (n=25)	
Edema	48 (53.93%)	18 (72.%)	0.326
Cystic Component	37 (41.57%)	13 (52%)	0.508
T1W			
Hypointense	73 (82.02%)	21 (84%)	0.871
Isointense	16 (17.97%)	4 (16%)	0.892
T2W			
Hypointense	4 (4.49%)	-	
Isointense	10 (11.23%)	4 (16%)	0.089
Hyperintense	75 (84.26%)	21 (84%)	0.917
DWI			
Hypointense	41 (46.06%)	11 (44%)	0.882
Isointense	25 (28.08%)	7 (28%)	0.958
Hyperintense	23 (25.84%)	7 (28%)	0.868
Contrast Enhancement			
Homogeneous	39 (43.82%)	7 (28%)	0.022
heterogeneous	50 (56.17%)	18 (72%)	0.041

*Group I: Invasive Ductal Ca, **Group II: Other Diagnostic Groups

The mean ADC value measured from the solid parts of the metastases was $1.105 \times 10^{-3} \text{mm}^2/\text{s}$ (0.705-1.678) in group 1 and $1.099 \times 10^{-3} \text{mm}^2/\text{s}$ (0.842-1.453) in group 2 ($p=0.931$). The mean ADC value in the normal brain parenchyma was measured as $0.790 \times 10^{-3} \text{mm}^2/\text{s}$ (0.683-0.852) in group 1 and $0.801 \times 10^{-3} \text{mm}^2/\text{s}$ (0.760-0.880) in group 2, respectively, and no significant difference was found ($p=0.452$) (Table 2).

Table 2. ADC levels of cases according to diagnostic groups

Variables	*Group I (n=89)	**Group II (n=25)	<i>p-value</i>
Solid ADC	1.105 (0.705-1.678)	1.099 (0.842-1.453)	0.931
Cystic ADC	2.012 (0.868-3.224)	2.542 (0.956-3.818)	0.274
Mixed ADC	1.450 (0.941-1.922)	1.745 (0.924-2.399)	0.246
Parenchyma ADC	0.790 (0.683-0.852)	0.801 (0.760-0.880)	0.452

*Group I: Invasive Ductal Ca, **Group II: Other Diagnostic Groups ADC: Apparent diffusion coefficient, ADC unit: $\times 10^{-3} \text{mm}^2/\text{s}^2$

In the evaluation of metastatic lesions according to their intensities on DWI, hypointensity was observed in 52 (45.61%) lesions, isointensity in 32 (28.07%) lesions, and hyperintensity in 30 (26.31%) lesions. Mean ADC values were measured as $1.218 \times 10^{-3} \text{mm}^2/\text{s}$ (0.874-1.453), $1.077 \times 10^{-3} \text{mm}^2/\text{s}$ (0.754-1.678), and $0.987 \times 10^{-3} \text{mm}^2/\text{s}$ (0.705-1.231), respectively. ADC values of hyperintense lesions were higher than isointensity and hypointensity ones significantly ($p=0.012$, $p<0.001$) (Table 3).

Table 3. Analysis of metastatic lesions according to their intensity on ADC map

Variables	ADC ($\times 10^{-3} \text{mm}^2/\text{sn}$)	<i>p-value</i>
Hypointense (N=52)	1,218 (0,874-1,453)	0.004
Isointense (N=32)	1,077 (0,754-1,678)	
Hypointense (N=52)	1,218 (0,874-1,453)	<0.001
Hyperintense (N=30)	0,987 (0,705-1,231)	
Hyperintense (N=30)	0,987 (0,705-1,231)	0.012
Isointense (N=32)	1,077 (0,754-1,678)	

ADC: apparent diffusion coefficient

The mean ADC values of the solid areas of the cases were higher in both groups (group 1: $1.105 \times 10^{-3} \text{mm}^2/\text{s}$ and group 2: $1.099 \times 10^{-3} \text{mm}^2/\text{s}$) than the normal brain parenchyma (group 1: $0.790 \times 10^{-3} \text{mm}^2/\text{s}$ and group 2: $0.801 \times 10^{-3} \text{mm}^2/\text{s}$) and were statistically significant ($p<0.001$) (Figure 2). In addition, in both groups, the mean ADC values of the solid areas (group 1: $1.105 \times 10^{-3} \text{mm}^2/\text{s}$ and group 2: $1.099 \times 10^{-3} \text{mm}^2/\text{s}$) were lower than the mean ADC values of the cystic areas (group 1: $2.012 \times 10^{-3} \text{mm}^2/\text{s}$ and group 2: $2.542 \times 10^{-3} \text{mm}^2/\text{s}$). ($p<0.001$) (Table 4) (Figure 3).

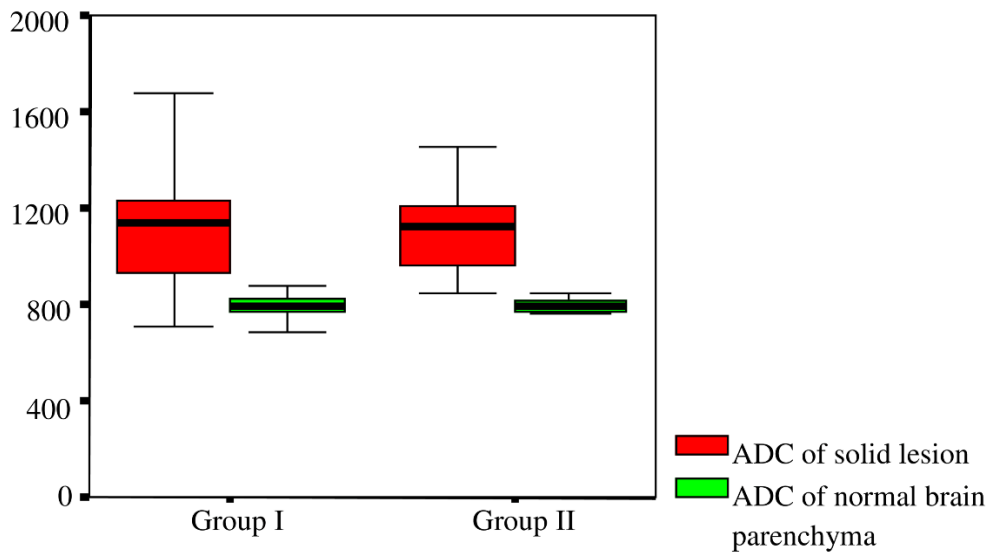
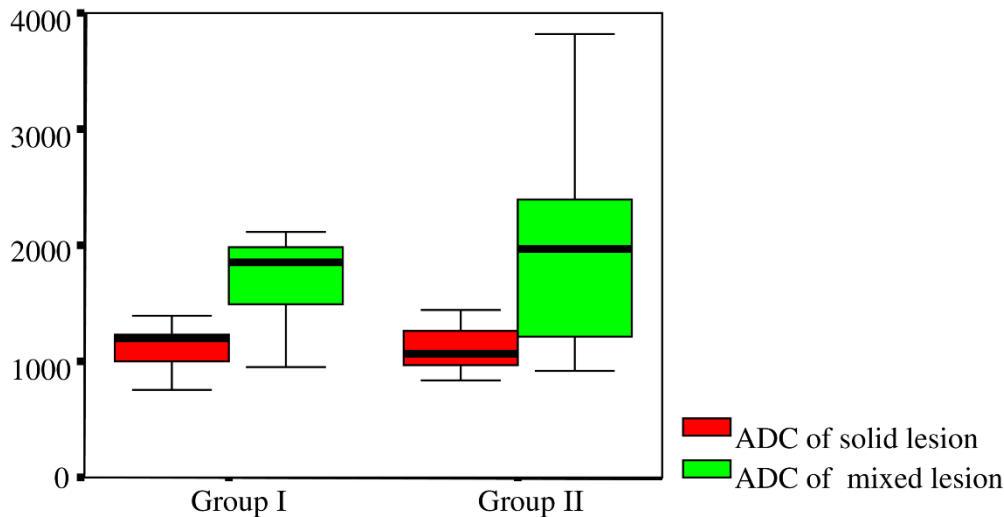


Figure 2. Distribution of mean ADC values of solid metastatic lesions and normal brain parenchyma in diagnostic groups (ADC unit: $10^{-6} \text{mm}^2/\text{s}$)

Table 4. Comparison of mean ADC levels of metastatic lesions and normal brain parenchyma between groups

Variables	*Group I (n=89)	<i>p value</i>	**Group II (n=25)	<i>p value</i>
Solid lesion and Mixed	1.105 (0.705-1.678)	<0.001	1.099 (0.842-1.453)	<0.001
	1.450 (0.941-1.922)		1.745 (0.924-2.399)	
Solid lesion and Normal Parenchyma	1.105 (0.705-1.678)	<0.001	1.099 (0.842-1.453)	<0.001
	0.790 (0.683-0.852)		0.801 (0.760-0.880)	
Solid lesion and Cystic lesion	1.105 (0.705-1.678)	<0.001	1.099 (0.842-1.453)	<0.001
	2.012 (0.868-3.224)		2.542 (0.956-3.818)	

*Group I: Invasive Ductal Ca, **Group II: Other Diagnostic Groups , ADC: Apparent diffusion coefficient, ADC unit: $\times 10^{-3} \text{mm}^2/\text{s}^2$

**Figure 3.** Distribution of ADC levels of solid and mixed lesions in diagnostic groups (ADC unit: $10^{-6} \text{mm}^2/\text{s}$).

DISCUSSION

In our study, mean ADC values of the lesions with cystic components were statistically significantly different than ADC values of normal white matter and solid metastatic lesions. Again, the ADC values measured on solid metastatic lesions were found to be significantly higher as compared to white matter. On DWI, ADC values were statistically significantly higher in hypointense cases as compared to isointense or hyperintense cases. However, no statistical difference in ADC values was found between the measurements of solid metastatic lesions and cystic lesions in 2 groups by histological type of breast cancer. The studies in the literature generally reported that mean ADC values were statistically higher on high degree tumors such as metastatic tumors and glioblastoma multiforme (GBM) as compared to mean ADC values on normal white matter. Its causes may include the presence of microcystic components on especially metastatic tumors and high degree glial tumors, the high risk of necrosis development, and increased extracellular fluid compartment.

It is not always possible to distinguish whether cystic or solid lesions occupying space in the brain belong to metastasis or not by conventional MRI or computed tomography. Diffusion weighted imaging offers some additional clues for distinction. Studies were showing a correlation between the stage of brain tumor and cellularity with the ADC values of tumor, generally it is reported that ADC values of high grade or cellularity tumors were lower than normal parenchyma. Tumor cellularity and tumor matrix leading to a difference in tumor histology contribute to the difference between ADC values (12-14). Water diffusion in biological tissues is highly dependent on intracellular and extracellular space ratio. The increased cellularity observed in high grade tumors decreases the extracellular space ratio. Accordingly, water diffusion decreases. Increased cellularity and mitotic activity on malign tumors decrease free diffusion rate of water, by increasing nucleus/cytoplasm ratio and the amount of intracellular complex protein molecules due to the features such as increased nucleus cytoplasm ratio, nucleoli prominence and necrosis. Therefore, increased cellularity ratio decreases extracellular space. Following this

biological event, it was considered that ADC values decreased especially on malign tumors without cystic component (15-18). In our study, mean ADC values were measured higher in solid metastatic lesions as compared to normal parenchyma, however, significantly lower as compared to cystic tumoral lesions. The result that the higher mean ADC values on solid metastatic lesions as compared to normal parenchyma might be associated with invisible microcystic structures, millimetric necrotic events and decreased tumor cellularity especially on the central sections where measurements were made.

In our study, we found that the mean ADC values of solid or cystic metastases were similar in both groups. When all cases and all measured lesions were included, the mean ADC value was $1.103 \times 10^{-3} \text{mm}^2/\text{s}$ in solid lesions and $2.128 \times 10^{-3} \text{mm}^2/\text{s}$ in cystic metastases. Compared to the normal parenchyma, higher ADC values were measured in all metastases and were statistically significant. Noguchi et al. (19) evaluated two pyogenic brain abscesses, 12 metastatic tumors and six high-grade glial tumors based on DWI features and ADC values. They found the mean ADC value of $0.94 \times 10^{-3} \text{mm}^2/\text{s}$ in 19 solid metastases due to lung and breast cancer and was consistent with the findings of our study. In the same study, the mean ADC value in the group consisting of 14 cystic metastases and necrotic tumors was $2.7 \times 10^{-3} \text{mm}^2/\text{s}$, which is similar to the mean ADC values of cystic metastases in our study (19). In a study performed by Hakyemez et al. (20), the DWI method was used to differentiate the necrotic tumors from brain abscess, and they found that DWI was hypointense since the internal structure of necrotic tumors were more serious as compared to abscess. They found the ADC values of necrotic tumors lower than cerebrospinal fluid (CSF) and higher than normal parenchyma and abscess. Besides, they reported that tumors and metastatic lesions having necrotic components were clearly hypointense on DWI trace images, but clearly hyperintense on ADC images. On 6 cystic metastatic cases, mean ADC value was measured as $2.82 \times 10^{-3} \text{mm}^2/\text{s}$ (1.56-3.12) (20). Santos et al. (21) compared brain MRI features according to histological subtype groups in their study of 147 cases with brain metastases due to breast cancer. Similar to our study, they reported that 111 (75.51%) of the patients did not have diffusion restriction on DWI and the signal was iso-hyperintense. However, ADC values were not measured in this study, and differences in histological subtypes were not studied (21).

The study performed by Yamasaki et al. (22) consisting of 275 cases with neuroepithelial and metastatic tumors was one of the largest series. In this study, it was found that mean ADC value was $1.149 \times 10^{-3} \text{mm}^2/\text{s}$ on metastatic lesions of 19 cases. However, the presence of cystic components in the metastatic lesions and the type of primary malignancy were not reported (22). In our study, similar to this study, the mean ADC values of solid metastatic lesions were $1.105 \times 10^{-3} \text{mm}^2/\text{s}$ in the group consisting of invasive ductal carcinoma, $1.099 \times 10^{-3} \text{mm}^2/\text{s}$ in the other group consisting of invasive lobular group.

In the study in which 36 GBM and 26 solid metastases were compared, the mean ADC values were higher in the GBM group, but no statistically significant difference was found between the two groups (23). In the same study, the mean ADC value was found to be $0.779 \times 10^{-3} \text{mm}^2/\text{s}$ in the

solid metastasis group, which is significantly lower than the value we found in our study. However, information on the origin of the metastases included in this study was not presented.

The most important limitation of our study is the combination of some subgroups histopathologically due to the small number of patients.

CONCLUSION

Diffusion Weighted Imaging and ADC measurements are important imaging methods for the diagnosis of intracranial tumors. Metastases in the brain parenchyma can show different signal characteristics in diffusion-weighted MRI. However, in our study, there was hypointensity in diffusion-weighted imaging in cystic metastases in accordance with the literature. Also, we found that ADC levels were higher in both cystic and solid metastatic lesions as compared to ADC levels in normal white matter. We did not find a correlation between the histological type of breast cancer and its metastatic lesion in terms of ADC measurement.

Authors's Contributions: Idea/Concept: Ş.K., N.Ç.; Design: Ş.K.; Data Collection and/or Processing: Ş.K.; Analysis and/or Interpretation: Ş.K., N.Ç.; Literature Review: Ş.K.; Writing the Article: Ş.K.; Critical Review: N.Ç.

REFERENCES

1. Custodio-Santos T, Videira M, Brito MA. Brain metastasization of breast cancer. *Biochim Biophys Acta Rev Cancer*. 2017; 1868(1): 132-47.
2. Saha A, Ghosh SK, Roy C, Choudhury KB, Chakrabarty B, Sarkar R. Demographic and clinical profile of patients with brain metastases: A retrospective study. *Asian J Neurosurg*. 2013; 8(3): 157-61.
3. Puac-Polanco P, Zakhari N, Miller J, McComiskey D, Thornhill RE, Jansen GH, et al. Diagnostic accuracy of centrally restricted diffusion sign in cerebral metastatic disease: differentiating radiation necrosis from tumor recurrence. *Can Assoc Radiol J*. 2023; 74(1): 100-9.
4. Romano A, Palizzi S, Romano A, Moltoni G, Di Napoli A, Maccioni F, et al. Diffusion weighted imaging in neuro-oncology: diagnosis, post-treatment changes, and advanced sequences-an updated review. *Cancers (Basel)*. 2023; 15(3): 618.
5. Alshoabi SA, Alkalady AH, Almas KM, Magram AO, Algaberi AK, Alareqi AA, et al. Hydatid disease: a radiological pictorial review of a great neoplasms mimicker. *Diagnostics (Basel)*. 2023; 13(6): 1127.
6. Gonçalves FG, Zandifar A, Ub Kim JD, Tierradentro-García LO, Ghosh A, Khrichenko D, et al. Application of apparent diffusion coefficient histogram metrics for differentiation of pediatric posterior fossa tumors: a large retrospective study and brief review of literature. *Clin Neuroradiol*. 2022; 32(4): 1097-108.
7. Phutharak W, Wannasarnmetha M, Lueangingsakut P, Warasawapati S, Mukherji SK. Differentiation between germinoma and other pineal region tumors

- using diffusion-and susceptibility-weighted MRI. *Eur J Radiol.* 2023; 159: 110663.
8. Kato H, Kawaguchi M, Ando T, Shibata H, Ogawa T, Noda Y, et al. Current status of diffusion-weighted imaging in differentiating parotid tumors. *Auris Nasus Larynx.* 2023; 50(2): 187-95.
 9. Srirambhatla A, Hosamani RD, Nandury EC. The role of diffusion-weighted imaging in the evaluation of adnexal lesions. *Pol J Radiol.* 2022; 87: e469-77.
 10. Broncano J, Steinbrecher K, Marquis KM, Raptis CA, Royuela Del Val J, Vollmer I, et al. Diffusion-weighted imaging of the chest: a primer for radiologists. *Radiographics.* 2023; 43(7): e220138.
 11. Fujii S, Gonda T, Yunaga H. clinical utility of diffusion-weighted imaging in gynecological imaging: Revisited. *Invest Radiol.* 2024; 59(1): 78-91.
 12. Fritz V, Martirosian P, Machann J, Thorwarth D, Schick F. Soy lecithin: A beneficial substance for adjusting the ADC in aqueous solutions to the values of biological tissues. *Magn Reson Med.* 2023; 89(4): 1674-83.
 13. Sugahara T, Korogi Y, Kochi M, Ikushima I, Shigematu Y, Hirai T, et al. Usefulness of diffusion-weighted MRI with echo-planar technique in the evaluation of cellularity in gliomas. *J Magn Reson Imaging.* 1999; 9(1): 53-60.
 14. Song Y, Yoon YC, Chong Y, Seo SW, Choi YL, Sohn I, et al. Diagnostic performance of conventional MRI parameters and apparent diffusion coefficient values in differentiating between benign and malignant soft-tissue tumours. *Clin Radiol.* 2017; 72(8): 691.e1-e10.
 15. Tyagi N, Riaz N, Hunt M, Wengler K, Hatzoglou V, Young R, et al. Weekly response assessment of involved lymph nodes to radiotherapy using diffusion-weighted MRI in oropharynx squamous cell carcinoma. *Med Phys.* 2016; 43(1): 137.
 16. Rahbar H, Partridge SC, Ha R. Editorial for "Stromal collagen content in breast tumors correlates with in vivo diffusion-weighted imaging: a comparison of multi b-value dwi with histologic specimen from benign and malignant breast lesions". *J Magn Reson Imaging.* 2020; 51(6): 1879-80.
 17. Ding Y, Tan Q, Mao W, Dai C, Hu X, Hou J, et al. Differentiating between malignant and benign renal tumors: do IVIM and diffusion kurtosis imaging perform better than DWI? *Eur Radiol.* 2019; 29(12): 6930-39.
 18. Choi YJ, Lee IS, Song YS, Kim JI, Choi KU, Song JW. Diagnostic performance of diffusion-weighted (DWI) and dynamic contrast-enhanced (DCE) MRI for the differentiation of benign from malignant soft-tissue tumors. *J Magn Reson Imaging.* 2019; 50(3): 798-809.
 19. Noguchi K, Watanabe N, Nagayoshi T, Kanazawa T, Toyoshima S, Shimizu M, et al. Role of diffusion-weighted echo-planar MRI in distinguishing between brain brain abscess and tumour: a preliminary report. *Neuroradiology.* 1999; 41(3): 171-4.
 20. Hakyemez B, Ergin N, Uysal S, Isik İ, Kilic E. Diffusion weighted MRI in brain abscess and necrotic tumor differentiation. *Diagn Interv Radiol* 2004; 10: 110-18.
 21. Santos J, Arantes J, Carneiro E, Ferreira D, Silva SM, Palma de Sousa S, et al. Brain metastases from breast cancer. *Clin Neurol Neurosurg.* 2020; 197: 106150.
 22. Yamasaki F, Kurisu K, Satoh K, Arita K, Sugiyama K, Ohtaki M, et al. Apparent diffusion coefficient of human brain tumors at MR imaging. *Radiology.* 2005; 235(3): 985-91.
 23. Zhang G, Chen X, Zhang S, Ruan X, Gao C, Liu Z, et al. Discrimination between solitary brain metastasis and glioblastoma multiforme by using adc-based texture analysis: a comparison of two different roi placements. *Acad Radiol.* 2019; 26(11): 1466-72.